Memory Effects Across Surfactant Mesophases

Donatella Capitani,[†] Anand Yethiraj,[‡] and E. Elliott Burnell*,[§]

Institute of Chemical Methodologies, CNR, Research Area of Rome, Via Salaria Km 29-300, Monterotondo Staz, Rome, Italy, Department of Physics and Physical Oceanography, Memorial University of Newfoundland, St. John's, Newfoundland A1B3X7, Canada, and Chemistry Department, University of British Columbia, 2036 Main Mall, Vancouver, British Columbia V6T 1Z1, Canada

We report a detailed analysis of deuteron NMR spectra of micellar, lamellar, cubic, and hexagonal mesophases in the aqueous non-ionic surfactant system $C_{12}E_6$/water. Samples are prepared with and without shear. Particular attention is paid to an interesting temperature-driven phase sequence that includes all of the above phases that are studied before and after shear parallel or perpendicular to the magnetic field direction. Surprising memory effects are found across mesophase transitions. These memory effects provide clues to the structure of the various phases.

1. Introduction

The $C_{12}E_6$/D_2O phase diagram (Figure 1, previously studied by many groups[1−4]) exhibits NMR-isotropic micellar and cubic phases as well as anisotropic lamellar and hexagonal phases. The structure of these phases has been studied extensively.[5−9] Although there are quantitative self-consistent estimates for the structure of the hexagonal phase[10,11] and the cubic phase,[12] the structure of the lamellar phase is still unclear.[7] The effect of shear on orientation provides an additional window into structure formation and has seen increasing interest.[13,14] Shear-induced transitions have been observed by NMR in the lamellar phase of $C_{12}E_6$/D_2O[15] and in the closely related $C_{12}E_4$ system.[16] In addition, NMR shear experiments in the hexagonal phase of $C_{12}E_6$/D_2O[17,18] and the related system $C_{12}E_5$[19] show that the hexagonal rods line up in the shear direction.

The $C_{12}E_6$/D_2O phase diagram of Figure 1 shows that there exists a surfactant concentration where all phases can be accessed by varying the temperature. We carefully study different samples, focusing on the ones prepared in this unique concentration
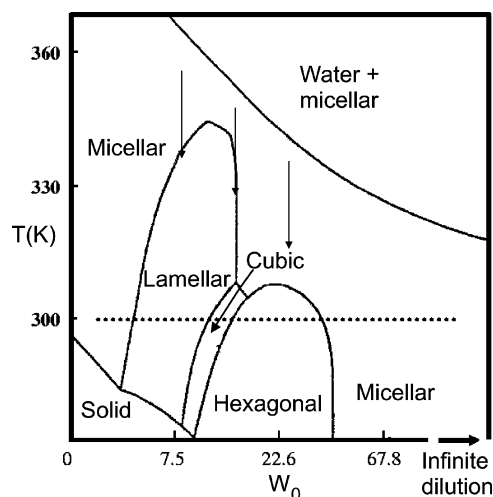

Figure 1. Phase diagram of aqueous solutions of $CH_3(CH_2)_{11}-(OCH_2CH_2)_6-OH$ as a function of molar ratios W_0 and temperature. Two-phase regions are not shown. Samples prepared at $W_0 = 7.8$, 15.0, and 23.0 (indicated by arrows) are reported in this work. At $W_0 = 7.8$, isotropic (above 334 K) and lamellar (below 332 K) phases are observed with a two-phase region between 332 and 334 K. At $W_0 = 23.0$, isotropic and hexagonal phases are observed. (All measurements were made at 300 K in the hexagonal phase.) At $W_0 = 15.0$, the phase sequence upon decreasing T is micellar (above 335 K), lamellar (between 333 and 307 K), cubic (between 302.5 and 295.5 K), and hexagonal (below 291.6 K), with two-phase regions observed at intermediate temperatures at each phase transition. The phase-transition temperatures changed slightly with time as a result of unavoidable water evaporation during the experiments.

[†] Institute of Chemical Methodologies, CNR.
[‡] Memorial University of Newfoundland.
[§] University of British Columbia.

(1) Tiddy, G. J. T. *Phys. Rep.* **1980**, *57*, 1.
(2) Mitchell, D. J.; Tiddy, G. J. T.; Waring, L.; Bostock, T.; McDonald, M. P. *J. Chem. Soc., Faraday Trans. 1* **1983**, *79*, 975.
(3) Fairhurst, C. E.; Holmes, M. C.; Leaver, M. S. *Langmuir* **1997**, *13*, 4964.
(4) Briganti, G.; Capitani, D.; Segre, A. L.; Casieri, C.; La Mesa, C. *J. Phys. Chem. B* **1999**, *103*, 825.
(5) Henriksson, U.; Klason, T. *J. Phys. Chem.* **1983**, *87*, 3802.
(6) Rançon, Y.; Charvolin, J. *J. Phys. Chem.* **1988**, *92*, 2646.
(7) Rançon, Y.; Charvolin, J. *J. Phys. Chem.* **1988**, *92*, 6339.
(8) Toledano, P., Figueiredo Neto, A. M., Eds. *Phase Transitions in Complex Fluids*; World Scientific: River Edge, NJ, 1998.
(9) Gaemers, S.; Bax, A. *J. Am. Chem. Soc.* **2001**, *123*, 12343.
(10) Constantin, D.; Oswald, P.; Impéror-Clerc, M.; Davidson, P.; Sotta, P. *J. Phys. Chem. B* **2001**, *105*, 668.
(11) Yethiraj, A.; Capitani, D.; Burlinson, N. E.; Burnell, E. E. *Langmuir* **2005**, *21*, 3311.
(12) Lindblom, G.; Rilfors, L. *Biochim. Biophys. Acta* **1989**, *988*, 221.
(13) Herb, C. A., Prud'homme, R. K., Eds. *Structure and Flow in Surfactant Solutions*; ACS Symposium Series 578; American Chemical Society: Washington, DC, 1994.
(14) Callaghan, P. T. *Rep. Prog. Phys.* **1999**, *62*, 599.
(15) Lukaschek, M.; Müller, S.; Hansenhindl, A.; Grabowski, D. A.; Schmidt, C. *Colloid Polym. Sci.* **1996**, *274*, 1.
(16) Müller, S.; Börschig, C.; Gronski, W.; Schmidt, C.; Roux, D. *Langmuir* **1999**, *15*, 7558.
(17) Lukaschek, M.; Grabowski, D. A.; Schmidt, C. *Langmuir* **1995**, *11*, 3590.
(18) Schmidt, G.; Müller, S.; Lindner, P.; Schmidt, C.; Richtering, W. *J. Phys. Chem. B* **1998**, *102*, 507.
(19) Müller, S.; Fischer, P.; Schmidt, C. *J. Phys. II France* **1997**, *7*, 421.
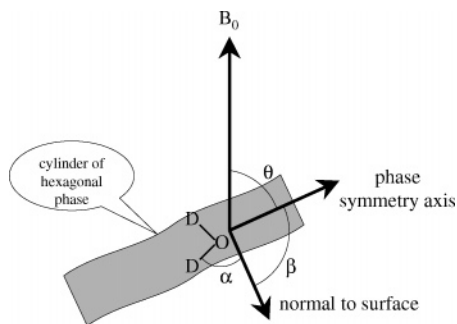
window, to shed light on and raise questions about structure and phase transitions.

Deuteron NMR and Order in Surfactant Mesophases. In an oriented phase composed of layers, the surfactant has an anisotropic influence on the water molecules. The water O−D bonds do not have a zero average order parameter (i.e., $S_{OD} \equiv \langle P_2(\cos(\alpha))\rangle \neq 0$, where α is the angle made by a water O−D bond with respect to the layer surface normal and the angle brackets denote an average). If the motions are fast enough to cause motional narrowing, then the splitting due to the quadrupolar interaction $\Delta\nu_Q$ is decreased by S_{OD}. If, in addition, the layers are curved and the diffusion of molecules along the surface is fast enough to cause motional narrowing, there is a further

Figure 2. Definition of axes and angles used in eqs 1−3 (using a cylinder of the hexagonal phase as an example).

reduction of $\langle P_2(\cos(\beta)) \rangle$ where β is the angle between the surface normal and the phase-symmetry axis.

The splitting due to the quadrupolar interaction is then approximated as

$$\Delta\nu_Q(\theta) = \frac{3}{2}\left(\frac{e^2qQ}{h}\right)S_{OD}P_2(\cos(\theta))\langle P_2(\cos(\beta)) \rangle \quad (1)$$

where θ is the angle between the phase-symmetry axis and the magnetic field direction B_0. (See Figure 2 for definitions of angles used.) For a planar lamellar phase, the surface normal is the phase-symmetry axis giving $\beta = 0$, and eq 1 becomes

$$\Delta\nu_Q(\theta) = \frac{3}{2}\left(\frac{e^2qQ}{h}\right)S_{OD}P_2(\cos(\theta)) \quad (2)$$

To simplify the discussion here, we ignore the asymmetry of the deuteron quadrupole tensor in D_2O.[20] Assuming axial symmetry about the O−D bond, we use a quadrupole coupling constant for the O−D bond of $e^2qQ/h \approx 220$ kHz.[21] S_{OD} varies with the surfactant/water molar ratio W_0 and is not known a priori because it is an average over the rapid exchange between the ordered surface-associated water and the varying pool of isotropic bulk water, whereas $P_2(\cos(\theta))$ varies from 1 when the layer normal is parallel to the magnetic field direction ($\theta = 0$) to $-(1/2)$ when the layer normal is perpendicular ($\theta = \pi/2$). Note that the deuteron on the water molecule is exchanging with the −OD of the surfactant head group on a time scale of a few milliseconds[22] and only a single average peak is observed.

In a hexagonal phase composed of cylinders, the surface normal makes an angle of $\beta = (\pi/2)$ with the cylinder axis, which is the phase-symmetry axis. With rapid diffusion about this axis, $\langle P_2(\cos(\beta)) \rangle = -(1/2)$ and eq 1 becomes

$$\Delta\nu_Q(\theta) = -\frac{1}{2}\frac{3}{2}\left(\frac{e^2qQ}{h}\right)S_{OD}P_2(\cos(\theta)) \quad (3)$$

where θ is now the angle between the cylinder axis and B_0. Note that throughout this article θ is the angle between the phase-symmetry axis (the cylinder axis for the hexagonal phase and the layer normal for the lamellar phase) and the magnetic field. There is convincing quantitative evidence[11,18,23,24] that the hexagonal phase is composed of undulating cylinders that are

(20) Abdolall, K.; Burnell, E. E.; Valic, M. I. *Chem. Phys. Lipids* **1977**, *20*, 115.

(21) Seelig, J. *Q. Rev. Biophys.* **1977**, *10*, 353.

(22) Geil, B.; Feiweier, T.; Pospiech, E.-M.; Eisenblatter, J.; Fujara, F.; Winter, R. *Chem. Phys. Lipids* **2000**, *106*, 115.

(23) Carvell, M.; Hall, D. G.; Lyle, I. G.; Tiddy, G. J. T. *Trans. Faraday Discuss.* **1986**, *81*, 223.

(24) Burnell, E. E.; Capitani, D.; Casieri, C.; Segre, A. L. *J. Phys. Chem. B* **2000**, *104*, 8782.

approximately 2 nm in diameter. These undulations are expected to reduce the value of $\langle P_2(\cos(\beta)) \rangle$ and consequently that of $\Delta\nu_Q(\theta)$.

In the hexagonal and lamellar phases, the observed spectrum contains sets of doublets for each orientation angle θ

$$\nu(\theta) = \nu_{Zeeman} \pm \frac{\Delta\nu_Q(\theta)}{2} \quad (4)$$

In an NMR-isotropic phase, an individual spin samples many orientations θ, and for a random distribution of orientations the motionally averaged value of $\langle P_2(\cos(\theta)) \rangle$ is 0, giving only a single peak at ν_{Zeeman}. A single-domain lamellar or hexagonal mesophase contains a single doublet (e.g., Figure 3D), whereas a random distribution of domains (a powder) exhibits the so-called Pake powder pattern that has singularities from domains oriented at $\theta = (\pi/2)$, referred to as the Pake doublet[25] (e.g., Figure 4A).

In a sample at fixed surfactant concentration, one might expect that S_{OD} changes little on crossing a phase transition. In this event, one expects the lamellar/hexagonal doublet splitting ratios to report directly on the relative average orientations. If these relative orientations are equal in both phases and if the fraction of surface-associated water remains constant, then we expect the same spectrum from a parallel-oriented hexagonal phase ($\theta = 0; \beta = 90°$) as for a perpendicularly oriented lamellar phase ($\theta = 90°; \beta = 0$).

In this article, we investigate the deuteron NMR spectra of the water component that experiences anisotropic interactions with the amphiphile surfaces and therefore reports on the order and nature of the amphiphile structures. We investigate the effect of shear that tends to orient the lamellar and hexagonal phases. We then monitor the effect of phase transitions on this order and hence investigate how the memory of this order is maintained across temperature-induced phase transitions. The sample of water to surfactant mole ratio $W_0 = 15.0$ is particularly interesting because it experiences all phases (micellar, lamellar, cubic, and hexagonal) as a function of changing temperature.

2. Experimental Section

Sample Preparation and Calibrations. $C_{12}E_6/D_2O$ samples were prepared as described in ref 4 with $C_{12}E_6$, $CH_3(CH_2)_{11}-(OCH_2-CH_2)_6OH$ (Tokyo Kasei, Japan, used as received), and D_2O (99.9%, used as purchased) at several compositions with different water-to-surfactant molar ratios W_0. Spectra were obtained from the Fourier transform of the free precession signal. Measurements were made on a "highly modified" Bruker CXP200 NMR spectrometer with a deuteron Larmor frequency of 30.72 MHz. Temperature was controlled to ± 0.5 K by a Bruker air-flow system. Free precession signals were digitized using a Nicolet 2090 digital oscilloscope and transferred to a PC for time averaging.

The shear experiments were performed with the apparatus described in ref 26 using 5 mm o.d. NMR tubes with solid glass rods of diameter 2 (narrow insert, N), 3, or 4 (wide insert, W) mm placed inside them. In some experiments, especially those utilizing a narrow glass rod, Teflon spacers were used above and below the NMR coil position to center the rod. The lower spacer fills the space at the bottom of the tube, ensuring that all of the sample is sandwiched between parallel glass cylinders whose symmetry axes are parallel to B_0. Perpendicular shear was applied (either manually or using a modified Tandon $5^1/_4$ in. floppy disk drive) by rotating the solid rod inside the NMR tube that was held stationary. Parallel shear was applied by raising and lowering the rod manually.

(25) Bloom, M.; Burnell, E. E.; Roeder, S. B. W.; Valic, M. I. *J. Chem. Phys.* **1977**, *66*, 3012.

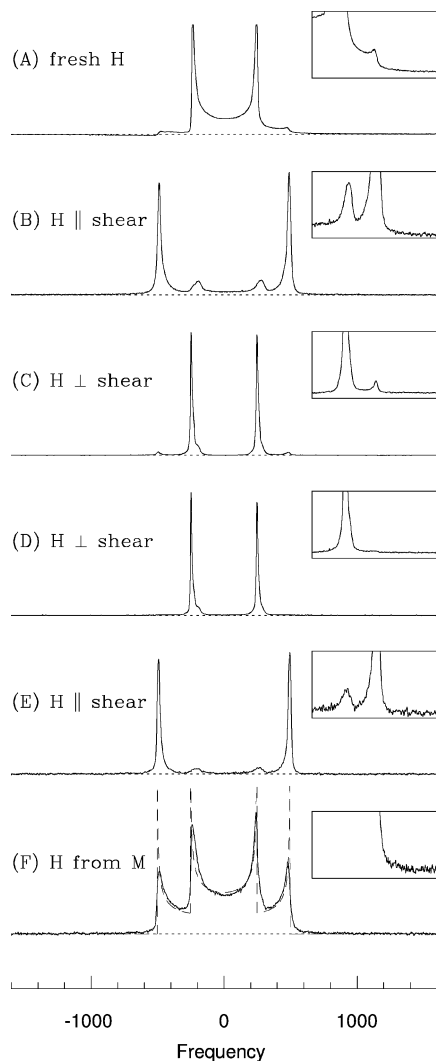(26) ter Beek, L. C.; Linseisen, F. M. *Macromolecules* **1998**, *31*, 4986.

Figure 3. Hexagonal-phase sample of composition $W_0 = 23.0$. The dotted lines are baselines and are intended to aid the eye in seeing the broad-line spectral intensity that is sometimes present in addition to the sharp peaks. The insets that show the right half of the spectra expanded vertically emphasize the broad-line component. Abbreviations used include M, micellar and H, hexagonal; fresh signifies a new sample that has not previously been in the magnetic field. (A) Freshly prepared sample at $W_0 = 23.0$, $T = 300$ K. The Pake doublet powder pattern is characteristic of a random distribution of domains. In this case, there is extra intensity (from extra parallel-oriented sample) at the outer edges of the spectrum. (B) Wide 4 mm insert W is inserted; $T = 300$ K. (C) Insert rotated 16 times by hand in the magnetic field; $T = 300$ K. (D) Insert rotated 64 times more. (E) Insert pushed up and down outside the magnet; $T = 300$ K. (F) The sample was heated to the micellar phase (at 310 K) and allowed to cool in the magnetic field into the hexagonal phase at $T = 300$ K. The dashed line indicates the calculated 2-D powder pattern with no line broadening; the four sharp peaks have infinite intensity and are truncated.

3. Results

NMR spectra of the D_2O component were obtained for several different concentrations in the phase diagram. We report results for concentrations $W_0 = 23.0$ in hexagonal and micellar phases, $W_0 = 7.8$ in lamellar and micellar phases, and $W_0 = 15.0$ in hexagonal, cubic, lamellar, and micellar phases.

3.1. Hexagonal Phase at $W_0 = 23.0$. Figure 3 reports spectra obtained in the hexagonal phase for a sample of composition $W_0 = 23.0$. A sample was freshly prepared in the hexagonal phase and placed into the magnet at 300 K (spectrum A). The Pake doublet powder pattern obtained is characteristic of a random
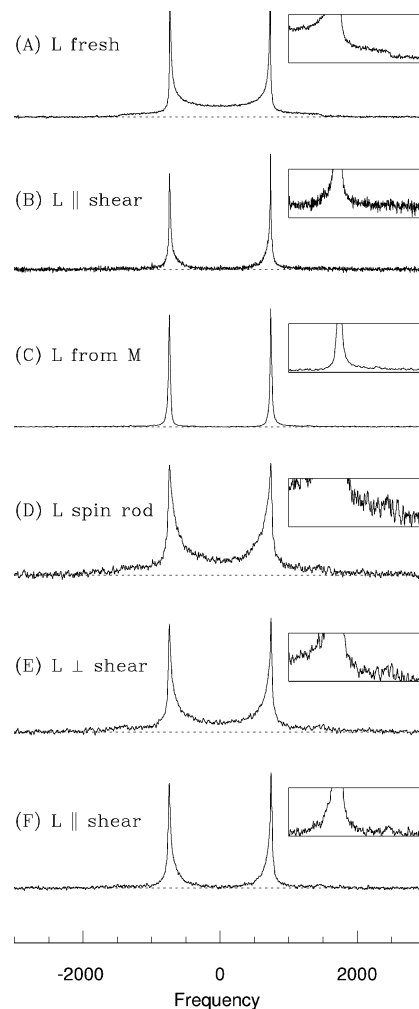

Figure 4. Lamellar-phase sample of composition $W_0 = 7.8$. Lamellar is abbreviated as L. (A) Freshly prepared sample. Wings characteristic of a powder spectrum are seen; $T = 300$ K. (B) Wide 4 mm insert W pushed into the NMR tube; $T = 300$ K. (C) Sample temperature raised to 343 K (micellar phase) and then cooled to $T = 300$ K. (D) Insert spinning at 1.1 Hz (shear rate 120 s^{-1}) by motor; $T = 300$ K. (E) Spectrum without spinning insert; $T = 300$ K. (F) Insert pushed up and down applying parallel shear in the magnetic field; $T = 300$ K.

orientational distribution of domains. (The extra intensity in the small "peak" visible at the right edge of the inset is from a small amount of a phase oriented parallel to B_0.) The 480 Hz splitting between the two "peaks" corresponding to the $\theta = 90°$ orientation of the phase-symmetry axis gives an order parameter of $S_{OD} = 0.0058$ using eq 3 (with respect to the layer normal, i.e., not including averaging associated with diffusion about the cylinders that make up the hexagonal phase). A 4-mm-diameter rod (wide insert W) was then placed into the sample tube, and the downward shear produced spectrum B. The major intensity now occurs with twice the splitting of the powder peaks (i.e., at the 0° edges of the powder pattern of A indicating that the sample is now relatively well oriented with the domain symmetry axes aligned along the magnetic field ($\theta = 0°$)). The $\theta = 90°$ peaks are shifted off center to the right by 40 Hz in this spectrum as they are also in E; this shift almost certainly arises from susceptibility effects associated with the different effective sample shape of the sample trapped between the bottom of the rod and the bottom of the NMR tube. For most of the sample, the symmetry axis of the hexagonal phase is aligned by the shear along the magnetic field direction. The insert is next rotated 16 times by hand, resulting

in C where the major intensity is now at the $\theta = 90°$ peaks of powder spectrum A. Thus the shear imposed by the rotation has aligned the cylinders perpendicular to the NMR tube and magnetic field. Further rotation (D) decreases the small $\theta = 0°$ component visible in C. The sample was removed from the magnet, and the insert was pushed up and down, resulting in alignment parallel to the tube axis and magnetic field (E, the small $\theta = 90°$ peaks are again shifted from the center of the spectrum). The alignment does not depend on whether the shear is performed inside or outside the magnetic field. Similar results are obtained for a $W_0 = 33.0$ hexagonal-phase sample with a narrower 3-mm-diameter insert.

Heating the sample into the micellar phase and then cooling in the magnet into the hexagonal phase results in a spectrum in which a large fraction of the cylinders are oriented parallel to the magnetic field as indicated by the excess intensity (compared to that of the random powder in A) at the 0° edges in F. This spectrum resembles the calculated (dashed line) 2-D powder pattern[27] that would result if cooling in the restricted area between the glass walls from the micellar phase resulted in all cylinders being oriented parallel to the glass walls with random values of θ, the angle between the cylinders and the magnetic field. Such a 2-D powder would have peaks at both the $\theta = 0$ and 90° positions in the spectrum.

The inner and outer doublets are symmetrically displaced about the spectral center, showing that susceptibility effects are absent and thus all signal arises from a single sample geometry.

Experiments (spectra not included) were also performed with the NMR tube axis perpendicular to the magnetic field. Pushing the insert up and down (perpendicular to B_0) aligns the hexagonal-phase cylinders perpendicular to the magnetic field. Insert rotation generates a 2-D powder pattern consistent with the cylinder axes being aligned perpendicular to the tube axis.

3.2. Lamellar Phase at $W_0 = 7.8$. Figure 4 reports spectra obtained from a lamellar-phase sample of composition $W_0 = 7.8$. A freshly prepared sample in the lamellar phase was placed into the magnet at 300 K (spectrum A). The Pake doublet powder pattern obtained arises from the random orientations of the director, which is normal to the lamellar plane. The wide insert W is then pushed into the tube (shear parallel to the magnetic field direction), and the sample becomes oriented with the layer normals perpendicular to the tube axis (and thus the magnetic field) as indicated by all spectral intensity being at the $\theta = 90°$ peak position (B), with splitting equal to 1473 Hz.

The sample is then warmed into the micellar phase at 343 K and cooled in the magnet into the lamellar phase at 300 K. The resulting spectrum (C) is that of a well-oriented sample with the director (which is normal to the planes) perpendicular to the magnetic field, as has been observed previously for similar samples.[4] Spectrum D is the spectrum taken while rotating the insert with respect to the outer NMR tube causing shear perpendicular to the magnetic field; the director orientation is frustrated by the spinning, and a distorted powder line shape is observed. On stopping spinning, the spectrum observed (E) is also a distorted powder pattern. Both D and E have more intensity near the $\theta = 90°$ peaks than does A, a random powder. However, there is a low-intensity signal for all θ values including $\theta = 0°$; perpendicular shear causes some of the sample to orient with the director aligned at various angles, including along the magnetic field.

The rod is now pushed up and down, causing parallel shear, and as in B, the sample becomes well aligned again (spectrum F). Hence perpendicular shear causes disorder in the D_2O director
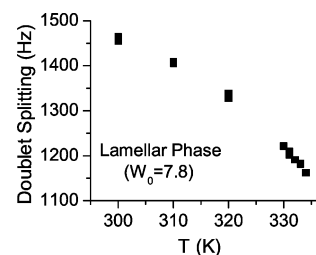
---

(27) Hentschel, R.; Sillescu, H.; Spiess, H. W. *Polymer* **1981**, *22*, 1516.

Figure 5. Doublet splitting in an oriented lamellar phase of composition $W_0 = 7.8$ varies by ~25% over a 30 K temperature range. Spectra acquired with wide 4 mm insert W spinning at 2.4 Hz.

with respect to B_0 (and thus the NMR tube axis), and parallel shear orients it perpendicular to B_0.

The doublet splitting obtained as a function of temperature while spinning the insert at 2.4 Hz (shear rate 250 s^{-1}) is given in Figure 5. A large variation with no hysteresis in the splitting is noted in the Figure. This variation is indicative of the lower orientational order of water at higher temperatures. The lower D_2O orientational order is almost certainly associated with the lower order of the $C_{12}E_6$ polar head groups as temperature increases.

3.3. Memory across Phase Transitions in a Four-Phase Sample ($W_0 = 15.0$). A particularly interesting composition in the phase diagram (Figure 1) is $W_0 = 15.0$, for which the micellar, lamellar, cubic, and hexagonal phases are accessible as a function of temperature. Many different experiments can be envisioned using this sample, and we report below several sequences of experiments that are particularly illuminating in terms of the physical nature of the $C_{12}E_6/D_2O$ system.

3.3.1. Heating following Parallel Shear: Hexagonal−Cubic− Lamellar Phase Sequence. Figure 6A is the spectrum of a freshly prepared sample of composition $W_0 = 15.0$ that was placed into the NMR probe at 293 K (spectrum is a mixture of hexagonal and cubic phases, not shown) and allowed to cool (from a mixture of cubic and hexagonal phases) to the pure hexagonal phase at 291.5 K. Unlike the hexagonal-phase $W_0 = 23.0$ sample, a Pake powder pattern is not obtained. The spectrum consists of a superposition of at least eight doublets of varying relative intensity.

The wide insert W is now pushed into the NMR tube (shear parallel to the magnetic field), and spectrum B is obtained. As was found for the $W_0 = 23.0$ sample (Figure 3B), shear parallel to B_0 orients a large fraction of the sample with the director or cylinder axes along the shear direction ($\theta = 0°$). The splitting between the larger or $\theta = 0°$ peaks is 1480 Hz, and that between the smaller residual peaks is 730 Hz (corresponding to a small amount of sample with $\theta = 90°$ orientation). As the sample is warmed to 292 K, a sharp peak appears in the center of spectrum C. This sharp or isotropic peak is from the formation of the cubic phase where the soap and water molecules diffuse about a bicontinuous cubic lattice; motional narrowing involving cubic symmetry leads to a single isotropic NMR line. At 296.5 K, the entire sample is in the cubic phase as indicated by the single, sharp NMR line in D. Upon further heating to 306 K, a coexistence of cubic and lamellar phases is observed (E), and at 308 K, the spectrum is entirely from the lamellar phase with a splitting of 685 ± 9 Hz (F). The lamellar phase (F) is fairly well oriented, but there is intensity between the peaks indicating that orientations in addition to $\theta = 90°$ exist; however, the spectrum is not consistent with a random powder but rather with a distribution of orientations with $\theta = 90°$ being favored.

It is noteworthy that the lamellar-phase splitting roughly equals the splitting for the $\theta = 90°$ hexagonal phase. Assuming that the
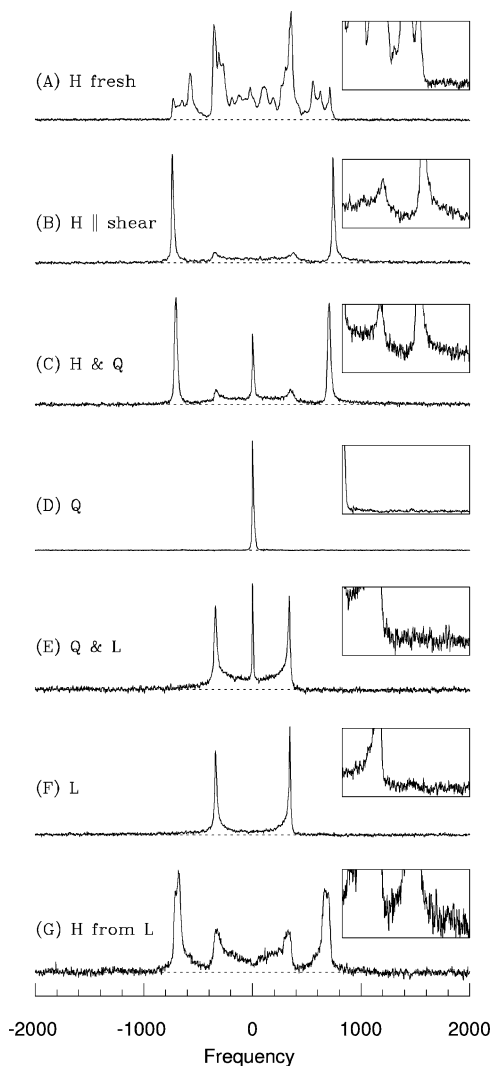
Figure 6. Sample of composition $W_0 = 15.0$ with 4 mm insert W. Cubic is abbreviated Q. (A) In a fresh sample, $T = 291.5$ K, the sample is hexagonal. The hexagonal-phase spectrum is not a powder spectrum but one that is partially oriented. (B) $T = 290$ K. Insert W has been pushed into the sample tube. Two sets of peaks are seen corresponding to splittings of 730 Hz (small peaks) and 1480 Hz (large peaks). The sample is thus mostly in the parallel orientation; see the text. (C) $T = 292$ K. The central peak signifies the appearance of the cubic phase. (D) $T = 296.5$ K, cubic phase. (E) $T = 306$ K, cubic−lamellar coexistence. (F) $T = 308$ K (lamellar); 685 ± 9 Hz peak splitting approximately equals the 730 Hz splitting of the perpendicularly oriented hexagonal phase (small peaks in B). (G) $T = 292$ K (cooled from $T = 308$ K). The hexagonal phase preserves much but not all of the parallel orientation.

lamellar phase is oriented with the normal perpendicular to B_0 ($\theta = 90°$, $\beta = 0$ in eq 1), a naive picture would predict the spectrum to be the same as that for the $\theta = 0°$ hexagonal phase ($\beta = 90°$) with the director parallel to B_0, as for the large peaks in B. In both cases, the normal to the $C_{12}E_6$ "planes" would lie perpendicular to B_0.

The fact that the lamellar-phase splitting is half that predicted is interesting and must be indicative of details about the structure of this lamellar phase. Rançon and Charvolin[7] also observed this reduced splitting and attribute it to the presence of hexagonal arrays of cylinders imbedded in the lamellar phase at low temperatures. Because the cylinder axes are expected to lie along B_0, their presence does not automatically lead to a reduced D_2O splitting because both lamellae and cylinders have surface normals perpendicular to B_0; the presence of the cylinders could be

associated with a decrease in the fraction of surface-associated water such that averaging between the surface-associated and bulk isotropic water leads to a reduction in D_2O splitting. We shall explore other possibilities below in section 4.

The opposite effect is observed in monoolein/water where the hexagonal is the higher-temperature phase and the D_2O has lower deuteron splitting than expected from the lamellar-phase spectrum. It is claimed that the reduction may be due to deviations from simple tubular topology or alternatively to lower lipid head group orientational order in the higher-temperature hexagonal phase.[28]

Spectrum G is obtained upon cooling the sample back through the cubic to the hexagonal phase at 292 K. Much of the parallel orientation of the hexagonal phase, as observed in B, has been retained upon heating the sample through the cubic to the lamellar and then back to the hexagonal phase. Hence there is partial memory across phase boundaries. However, it should be noted that there is an increased powder contribution present in G compared to that in C.

3.3.2. Perpendicular Shear and the Hexagonal−Cubic− Hexagonal−Lamellar Sequence (Figure 7). The rod insert in the hexagonal-phase sample that gave the spectrum of Figure 6G is now rotated, applying shear perpendicular to B_0, and as was the case for the $W_0 = 23.0$ sample (Figure 3), the director aligns perpendicular to B_0 as demonstrated by the $\theta = 90°$ peaks with 720 Hz splitting in Figure 7A.

The sample is then heated to 298 K in the cubic phase, giving the sharp isotropic peak of spectrum B, and then cooled back to the hexagonal phase at 292 K (spectrum C). The spectrum is still dominated by the $\theta = 90°$ peaks signifying that transition into the cubic phase does not result in loss of memory of the original orientation in the lower-temperature hexagonal phase. However, we note the increased intensity of the $\theta = 0°$ edges in C. When the experiment in A−C is repeated using a narrower insert (spectrum not shown), the increase in intensity at the $\theta = 0°$ edges is more pronounced and is accompanied by increased intensity for other angles as well. A similar result is obtained for a sample oriented by parallel shear in the hexagonal phase and cycled through the cubic phase: the parallel $\theta = 0°$ peaks remain dominant (spectrum not shown) with an increase in intensity for signal from other angles. Hence cycling through the cubic phase results in maintaining the original orientation of the hexagonal phase for much of the sample but with additional orientation directions being observed upon returning to the hexagonal phase.

On heating to the lamellar phase (D), the sample remains somewhat oriented but with a distribution of orientations as observed in Figure 6F. As also observed in Figure 6, the 681 Hz splitting observed in D is very close to the 720 Hz splitting of the hexagonal phase in A. Figures 6 and 7 show that both parallel and perpendicular orientations of the hexagonal phase lead to essentially the same lamellar-phase spectrum. The distribution of orientations found in the lamellar phase must result from passing the sample (oriented in the hexagonal phase) through the cubic phase.

3.3.3. Micellar−Lamellar−Cubic−Hexagonal Cooling Sequence (Figure 8). Next we examine the cooling of the $W_0 = 15.0$ sample from the micellar phase through the lamellar and cubic phases to the hexagonal phase. The micellar phase gives a sharp, isotropic peak that results from motional narrowing due to the isotropic tumbling of the micelles (Figure 8A). This isotropic motion means that memory of any earlier orientational effects is erased by being in the micellar phase. The coexistence of micellar and lamellar peaks is observed at 330 K (B). The lamellar

(28) Feiweier, T.; Geil, B.; Pospiech, E.-M.; Fujara, F.; Winter, R. *Phys. Rev. E* **2000**, *62*, 8182.
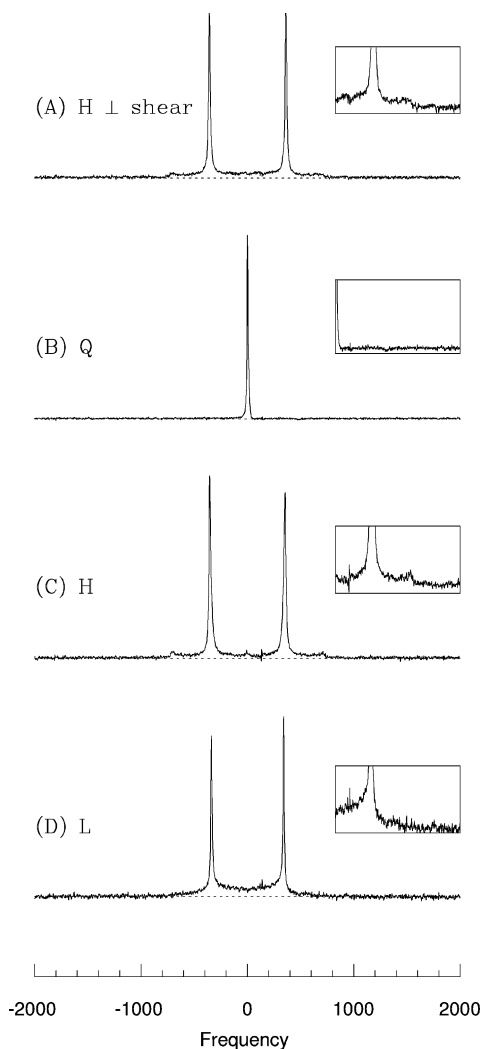
Figure 7. Sample of composition $W_0 = 15.0$ with 4 mm insert W. (A) $T = 292$ K. The insert was rotated 180° (forward and back) in the hexagonal phase to obtain a perpendicularly oriented hexagonal phase. (B) It was then heated into the cubic phase ($T = 298$ K). A single isotropic peak is seen. (C) The sample was cooled back to $T = 292$ K (into the hexagonal phase). The perpendicular orientation was preserved! (D) The sample was warmed to $T = 306$ K, lamellar phase, with 681 Hz splitting corresponding to the perpendicular orientation of the lamellar phase.

Figure 8. Sample of composition $W_0 = 15.0$ with 4 mm insert W. (A) $T = 335$ K (micellar). (B) $T = 330$ K (coexistence of micellar phase with lamellar phase with 725 Hz doublet splitting corresponding to perpendicular orientation). (C) $T = 320$ K (lamellar). (D) $T = 306$ K (lamellar−cubic coexistence); lamellar-phase splitting is 681 Hz. The integrated intensity of the cubic-phase peak is 7% that of the lamellar-phase peaks in both this spectrum and the one recorded for the same sample at the same temperature in Figure 6E. (E) $T = 303$ K (cubic). (F) $T = 293$ K (hexagonal). The lamellar phase is oriented, but the hexagonal phase has several doublets with the two major ones having splittings of 676.5 and 1391.6 Hz. (i.e., perpendicular and parallel orientations). Note that the doublet splitting in the lamellar phase shows a temperature dependence, with the larger splitting being observed at the higher temperature.

phase cooled from the micellar phase consists of two sharp peaks (splitting 725 Hz) indicative of the sample being oriented with the director perpendicular to B_0 as observed in Figure 4C for the $W_0 = 7.8$ lamellar-phase sample. Further cooling gives pure lamellar-phase spectrum C, and eventually at 306 K the coexistence of the lamellar-phase doublet (splitting 681 Hz) and cubic-phase isotropic peaks is observed (D).

Unlike the $W_0 = 7.8$ sample for which the lamellar peak splitting decreases with increasing temperature (Figure 5), it increases for the $W_0 = 15.0$ sample. In other words, the D_2O order parameter increases with increasing temperature. This phenomenon has been observed with monoolein/water lamellar phases[28] and with potassium palmitate/D_2O lamellar phases. In the latter case, it was ascribed to changes in the direction that the polar head makes with the surface normal.[20] It has also been observed previously in this system ($C_{12}E_6$) and was ascribed to a reduction with increasing temperature in the concentration of hexagonal arrays of cylinders that are proposed to be imbedded in the lamellar phase at temperatures just above the cubic/lamellar phase transition.[7]
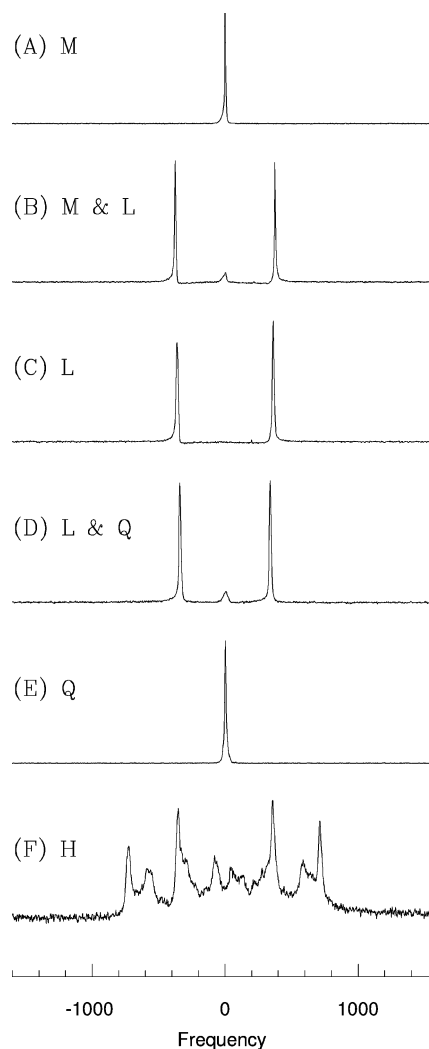
The spectrum at 303 K is the isotropic peak of the cubic phase (E). Further cooling to 293 K gives the hexagonal-phase spectrum (F). The hexagonal phase is not a powder but a collection of peaks (a pseudopowder). Note that cooling with no shear to the hexagonal from the micellar through the lamellar and cubic phases gives unusual splittings, and the spectrum is similar to that observed in Figure 6A for the same sample when freshly prepared and placed into the magnet with no shear.

Spectrum F also resembles the spectrum observed by Henriksson and Klason[5] upon slow cooling from the micellar phase in the magnetic field with the exception that there is an additional doublet at the parallel $\theta = 0°$ edges in our spectrum. Henriksson and Klason observed four doublets and studied the change in spectral splittings as a function of sample rotation angle. They claim that the results are consistent with the resulting hexagonal phase being composed of a tetrahedral arrangement of hexagonal
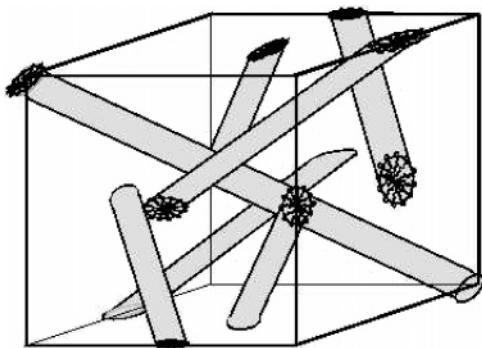
Figure 9. Cartoon of the cubic phase composed of interconnecting cylinders. There are four sets of parallel cylinders, and the angle between each set of non-parallel cylinders is the tetrahedral angle. The interconnects between cylinders are not shown. From reference 11.

directors initially oriented with one director perpendicular to B_0 ($\theta = 90°$) and with a second at $\theta = 19.47°$. It is proposed that the crystallites of the hexagonal phase grow from the tetrahedral directions of the structure of the cubic phase (depicted in Figure 9). As discussed in section 3.4 on orientational oddities, we often observe one or more sets of four doublets that are consistent with tetrahedral arrangements of hexagonal directors and are therefore consistent with the hexagonal cylinders growing from the tetrahedral directions of the cubic phase. However, we do not always find that one of the directions is perpendicular to B_0 ($\theta = 90°$); see below.

3.3.4. Hexagonal Phase Remembers Shear in the Lamellar and Cubic Phases (Figure 10). The insert is rotated to apply perpendicular shear to the $W_0 = 15.0$ sample in the hexagonal phase at 290 K, and a $\theta = 90°$ doublet with 728 Hz splitting is observed (Figure 10A). The sample is heated to the lamellar phase at 308 K, and a doublet of 689 Hz splitting is observed with some powderlike intensity between the peaks (B). These results are consistent with the observations of Figure 7. The insert is rotated to apply perpendicular shear to the sample in the lamellar phase (C). As was the case for the $W_0 = 7.8$ sample (Figure 4E), the sample shows evidence of some random orientations as indicated by the increase in signal intensity between the $\theta = 90°$ peaks as well as some intensity outside these peaks. The insert is now pushed up and down, applying parallel shear, and a doublet of 685 Hz splitting indicative of a well-oriented sample results (D). The sample is next cooled through the cubic phase to the hexagonal phase at 291 K where spectrum E contains a sharp doublet of 1444 Hz splitting indicative of $\theta = 0°$ (i.e., with the director parallel to B_0). There is extra intensity between the $\theta = 90°$ peaks indicating that other orientations are present. However, it is interesting that the effect of parallel shear applied to the lamellar phase results in parallel orientation in the lower-temperature hexagonal phase, with the memory of the shear direction being retained. This is evidence that both hexagonal- and lamellar-phase structures are related to the structure of the cubic phase that connects them. Cooling to 293 K in the hexagonal phase after spinning with the motor to apply perpendicular shear in the lamellar phase at 310 K gives spectrum F. The 0° peaks are still quite pronounced but are of lower integrated intensity (and the 90° peaks are of greater intensity) than in spectrum E. There is intensity at other angles, and the weighting of the 90° peaks is less than would result from a random powder. However, the differences between E and F clearly show that the direction of shear in the lamellar phase contributes intensity to the hexagonal-phase signal associated with hexagonal cylinders aligning along the lamellar-phase shear direction. Finally, rotation
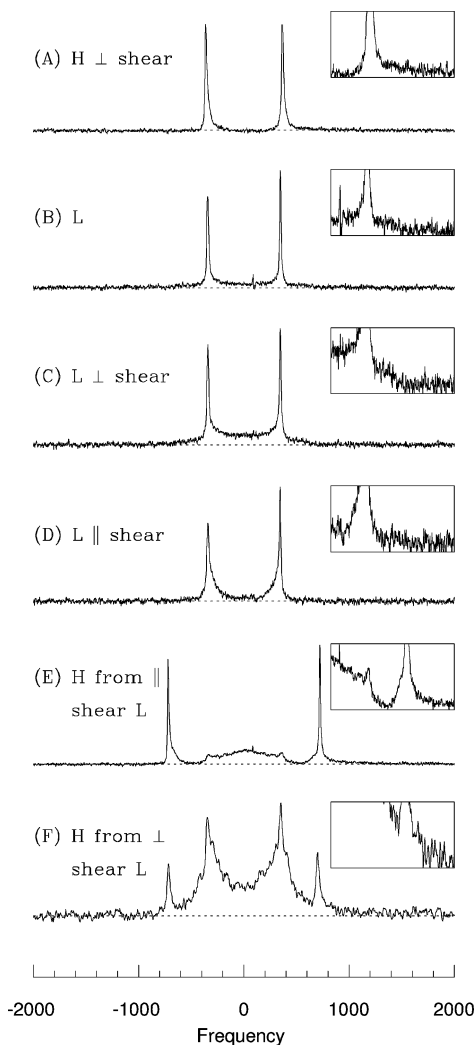

Figure 10. Sample of composition $W_0 = 15.0$ with 4 mm insert W. (A) $T = 290$ K (hexagonal, insert rotated, 727.8 Hz splitting). (B) $T = 308$ K (warmed to lamellar, 688.7 Hz splitting). (C) $T = 308$ K (lamellar, insert rotated, 685.1 Hz splitting). (D) $T = 308$ K (lamellar, insert pushed up and down, 685.1 Hz splitting). (E) $T = 291$ K (cooled to hexagonal, 1443.5 Hz splitting). (F) $T = 293$ K (cooled to hexagonal after spinning with motor at 0.8 Hz in the lamellar phase at 310 K).

of the insert providing perpendicular shear to the hexagonal-phase sample at 291 K gives an oriented sample spectrum similar to A with a doublet of 722 Hz splitting.

The $W_0 = 15.0$ sample with the wide insert W remembers its orientation when the temperature is changed from one phase to another.

3.3.5. Thicker Samples (Narrow 2-mm-Diameter Insert N). To assess the importance of surface interactions on the effects described above, spectra were obtained from samples exposed to shear using a narrower rod (insert N) of diameter 2 mm inside a 5 mm o.d. NMR tube. A Teflon spacer held the rod in the center at the bottom of the tube, and a Teflon spacer placed above the NMR coil kept the rod centered along the tube. The bottom spacer filled the volume of the NMR tube below the rod, thus removing possible signal artifacts from sample not exposed to shear or exposed to shear between the rod and tube bottom.

Figure 11A is the spectrum of a fresh sample of composition $W_0 = 15.0$ in the hexagonal phase at 289 K, and the pseudopowder spectrum observed is similar to yet different from those observed in Figures 6A and 8F. The sample is heated through the cubic phase to the lamellar phase at 310 K, and a powder pattern with
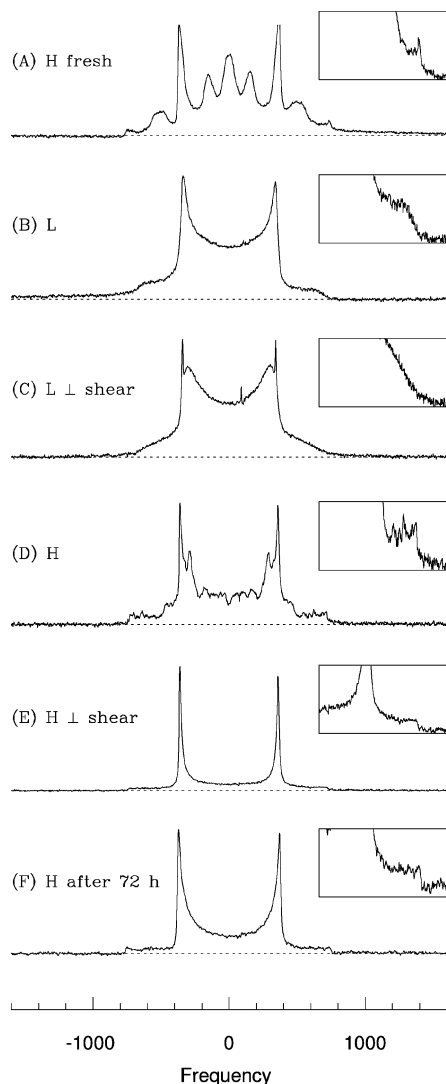
Figure 11. Spectra from the $W_0 = 15.0$ sample with the 2 mm insert N. (A) Fresh sample, cooled to $T = 289$ K (hexagonal phase). A pseudopowder pattern signifying partial orientation is observed. (B) $T = 310$ K. Sample has been heated into the lamellar phase, and a powder pattern is seen. (C) $T = 310$ K. The insert was spun in the lamellar phase, spectrum after spinning stopped. (D) $T = 292$ K. Cooled to the hexagonal phase. (E) $W_0 = 15.0$ sample at $T = 292$ K (hexagonal phase) after insert rotated applying perpendicular shear. (F) After 72 hours ($T = 287$ K), less orientation is observed.

Figure 12. $W_0 = 15.0$ sample with the 2 mm insert N. (A) $T = 336$ K (micellar). (B) $T = 325$ K (lamellar). (C) $T = 290$ K (hexagonal). (D) The sample insert was spun by motor in the cubic phase at $T = 300$ K, and the sample was then cooled with a stationary insert to the hexagonal phase; $T = 289$ K.

no observed fine structure is observed (B). It is interesting that the pseudopowder spectrum in the hexagonal phase (from a "fresh" sample) results in a true powder pattern in the lamellar phase. Indeed, simply cycling a micellar-phase sample through the lamellar phase (where it becomes oriented) into the cubic phase and back to the lamellar phase also results in a powder lamellar-phase spectrum (not shown).

Rotation of the insert (shear perpendicular to B_0) in the lamellar phase gives spectrum C. This Figure is essentially the superposition of a sharp doublet from domains oriented at $\theta = 90°$ (presumably near surfaces) and a powder. Spectrum D is observed upon cooling through the cubic to the hexagonal phase at 292 K; a pseudopowder spectrum is observed, but it differs in detail from A and also from that in Figure 10F in that the 0° peaks are less pronounced. The insert is now rotated in the hexagonal phase at 292 K, and the superposition of a $\theta = 90°$ doublet with remnants of a powder spectrum is observed (E). This sample was also used to demonstrate that the orientational distribution is not necessarily an equilibrium distribution. This is demonstrated in
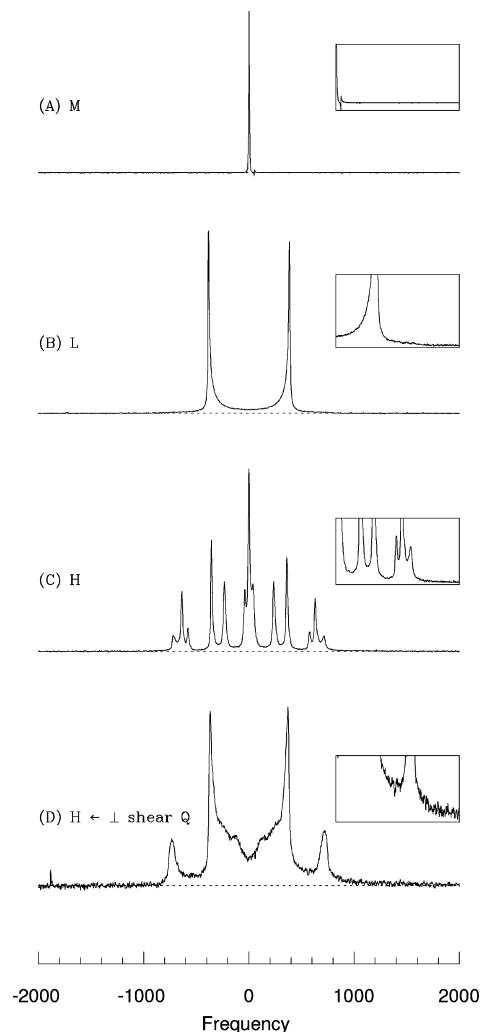
F, which shows that the spectrum of the $W_0 = 15.0$ sample in the hexagonal phase (E) changes over 72 h, as indicated by the increase in spectral intensity with time between the peaks in F: the director orientations are becoming more random with time.

Figure 12 is another example of cooling the $W_0 = 15.0$ sample from the micellar (A) through the lamellar (B) and cubic phases to the hexagonal phase (C). This sample contained the narrow shear rod N, but the spectra were obtained in the absence of any shear. As before (Figure 8), the lamellar-phase spectrum is a sharp doublet from a well-oriented sample with the director perpendicular to B_0 but with some powder contribution not present in Figure 8. Perhaps wall effects are less important with the increased spacing between walls in this sample that uses a narrow rod. This time the pseudopowder spectrum (C) of the hexagonal phase consists of at least seven sharp doublets, indicating that only certain domain orientations are allowed.

The sample is now warmed to the cubic phase at 300 K, and the narrow shear rod N is spun at 1.25 Hz (shear rate 8 s^{-1}) using the motor. Spinning is stopped, and the sample is cooled to the hexagonal phase at 289 K, giving spectrum D. The spectrum is a curious quasi-powder and has a lot of intensity at both $\theta = 0$ and 90° orientations. Although the extra intensity is not associated with sharp peaks as observed in Figure 12C, some θ angles are preferred. In particular, $\theta = 0°$ is highly favored over the intensity
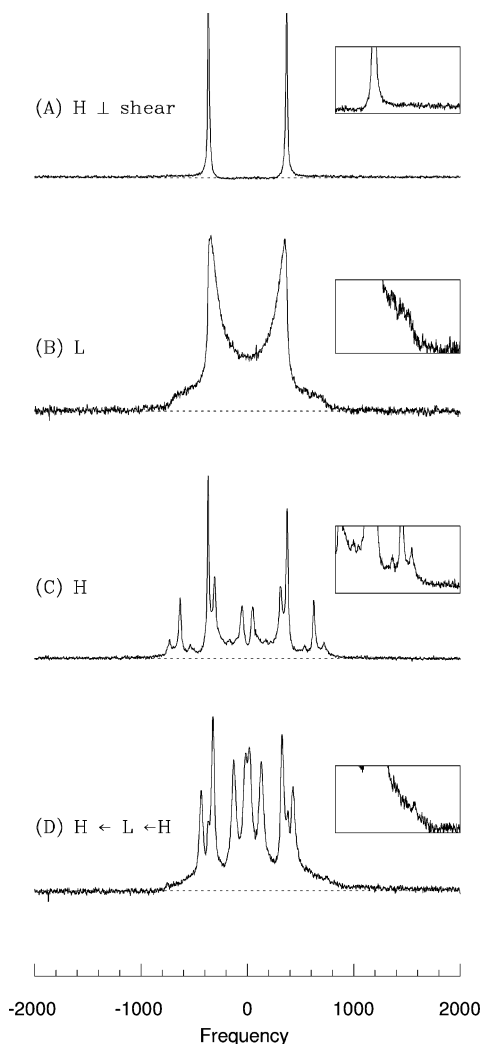
Figure 13. $W_0 = 15.0$ sample with the 2 mm insert N. (A) The sample insert was spun by motor at $T = 290$ K (hexagonal). The spectrum was obtained with spinning off. (B) Sample warmed to $T = 310$ K. The lamellar phase is a distorted powder. (C) $T = 289$ K; cooled to the hexagonal phase. (D) Sequence A–C repeated. Spectrum at $T = 289$ K.

expected for a random powder. The large $\theta = 0°$ peaks in spectrum D are reminiscent of those in the 2-D powder pattern (similar to Figure 3F) that would result from a random distribution of cylinder axes lying in a plane whose normal is perpendicular to B_0. The shear in the cubic phase appears to destroy the memory of the orientation in the hexagonal phase and to encourage somewhat cylinders to align with their axes parallel to the glass walls. Hence, applying perpendicular shear in the cubic phase prior to cooling into the hexagonal phase destroys the memory.

Rotating insert N at 1.25 Hz to apply perpendicular shear to the $W_0 = 15.0$ sample in the hexagonal phase at 289 K gives a sharp doublet associated with domains oriented perpendicular to B_0 (Figure 13A). Raising the temperature through the cubic to the lamellar phase gives a powder spectrum (B) that is consistent with that for the thin sample (Figures 7D and 10B). B is not a perfect powder pattern with $\theta = 90°$ being favored, but $\theta = 90°$ is not favored as much as for the thin sample. Subsequent cooling into the hexagonal phase gives a pseudopowder (C). Note that different runs of the identical experiment give identical lamellar powders but the detailed spectrum of the pseudopowder changes (compare C and D). Most of the memory of the original orientation in the hexagonal phase is now lost. However, in both C and D there are $\theta = 90°$ peaks present (at ± 371 Hz in C and the small

shoulders at ± 375 Hz in D). Therefore, the perpendicular hexagonal axis is preserved for some of the cylinders. In C, this axis is one of four that describe a tetrahedral arrangement of cylinders (the other three axes being associated with the six additional larger peaks). In D, the larger peaks also are consistent with a tetrahedral arrangement of cylinders; however, the $\theta = 90°$ shoulders are not part of this set. In this case, most of the perpendicular cylinders are shifted somewhat from their original orientation, and memory has been lost.

Comparing the spectra in Figures 11–13 (which use narrow insert N) with those in Figures 6–10 (which use wide insert W) demonstrates that memory effects are more pronounced in thinner samples where wall effects might be expected to dominate. The absence of convection-induced disordering in the thin samples might be important in preserving memory effects.

3.4. Orientational Oddities and the Hexagonal Pseudopowder Spectrum: Partial Orientation in the Hexagonal Phase in the $W_0 = 15.0$ (Four-Phase) Sample. The strange pseudopowder spectra observed in the hexagonal phase of the $W_0 = 15.0$ sample are further explored in Figure 14, where several additional examples are presented. Cooling from the micellar phase, or from a lamellar phase, gives different pseudopowder spectra each time.

In most cases where multiple sets of peaks are observed in the hexagonal phase, at least one set of four doublets can be rationalized as arising from a set of tetrahedrally arranged cylinders. To be consistent, sets of four couplings from a pseudopowder spectrum must have a sum of zero to reflect the isotropic peak observed in the cubic phase (where motional narrowing among tetrahedrally packed cylinders leads to a single motionally averaged peak). In performing the addition, one must allow all possible signs of the splittings, with the restriction that any splitting greater than that of the $\theta = 90°$ value must be positive. Spectra C (the central peak is one doublet) and E (the central peak is not included because it is a remnant of the cubic-phase spectrum), both cooled from the micellar phase in the magnetic field, are consistent with two tetrahedra that are oriented differently with respect to B_0 and are oriented differently in the two samples.

The picture that emerges and that is consistent with earlier observations[5,7] is that the cubic phase consists of a tetrahedral arrangement of interconnected cylinders as depicted in Figure 9 and that when the hexagonal phase is formed the cylinders grow along one of the cylinder directions of the cubic phase. The presence of a limited number of directions indicates that the cubic phase in our experiments is composed of a very small number of single crystals (one or two). Unlike earlier experiments where very slow cooling from the micellar phase was employed,[5] we do not obtain a single orientation of the cubic phase; however, we do obtain a limited number of crystal orientations, and their orientations vary when repeating the experiment. This variation in tetrahedral orientations is demonstrated in Figure 15 where the tetrahedral angles calculated from the spectral peak positions in 26 experiments are reported. The variation in angles among samples must be associated with a lack of influence on the growth direction of the cylinder axes in our experiments. Earlier experiments using slow cooling[5] do report definite cylinder directions.

In a few experiments (not shown), especially those using insert W, the hexagonal-phase spectrum in the $W_0 = 15.0$ sample is reminiscent of the two-dimensional powder observed for the $W_0 = 23.0$ hexagonal-phase sample (Figure 3F) with $\theta = 0$ and $90°$ peaks. In these instances, the close proximity of the walls may be determining the growth direction of the hexagonal from the cubic phase such that the cylinders lie along the wall surface.
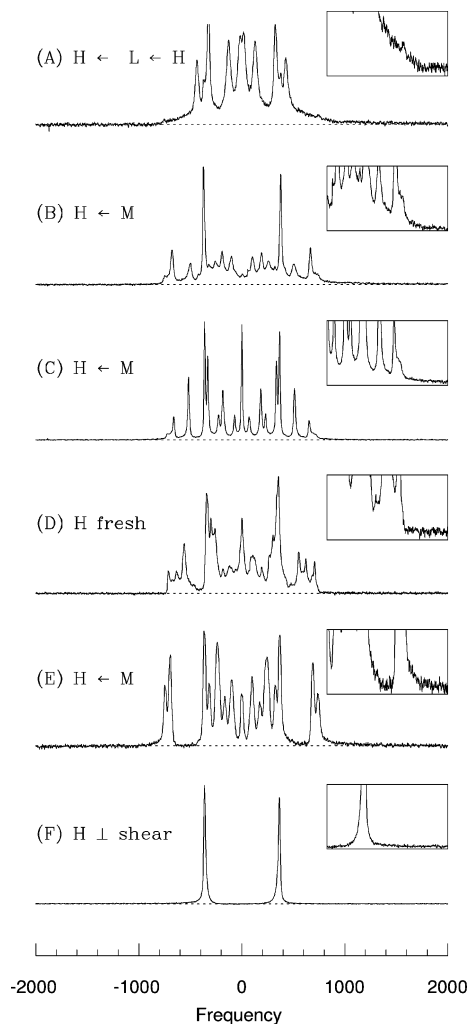
Figure 14. Partial orientation of the $W_0 = 15.0$ sample in the hexagonal phase; all used 2 mm insert N except D, which used insert W. The sharp peaks at the origin in spectra C–E are from a small amount of cubic phase in coexistence with the hexagonal phase. (A) Figure 13D repeated—perpendicular shear in the hexagonal phase, heated to the lamellar phase (distorted powder pattern observed), and then cooled to $T = 289$ K. (B) Sample in the magnet at 337 K (micellar), cooled to 300 K (cubic), annealed at 300 K for 12 hours, and then cooled to $T = 289$ K. (C) Sample cooled in the magnet from the micellar phase; $T = 294$ K. (D) $T = 293$ K, freshly prepared sample (using insert W). (E) $T = 291$ K, sample cooled from the micellar phase. (F) $T = 290.5$ K, spectrum taken with the insert spinning at 1.25 Hz applying perpendicular shear at 8 s⁻¹.

Spectrum F in Figure 14 reminds us that shear does orient the domains in the hexagonal phase (in this case, perpendicular with perpendicular shear) and is provided as a reference.

4. Discussion

4.1. Structure of the Hexagonal Phase. In the hexagonal phase, we notice the following:

• Up–down shear results in a spectrum composed of a doublet with ∼1400 Hz splitting in $W_0 = 15.0$ and ∼980 Hz splitting in $W_0 = 23.0$. The smaller splitting in $W_0 = 23.0$ reflects the larger amount of bulk, isotropic D_2O in this sample. Up–down shear is consistent with $\theta = 0°$ and $\beta = 90°$ in eq 1.

• Rotary shear results in a spectrum composed of a doublet with ∼700 Hz splitting in $W_0 = 15.0$ and ∼480 Hz splitting in $W_0 = 23.0$, being half the values for parallel shear. The reduction arises from cylinders becoming oriented perpendicular to B_0 (i.e., in this case $\theta = 90°$ and $\beta = 90°$ in eq 1).
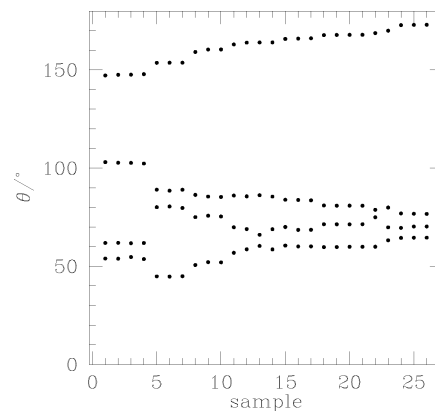

Figure 15. Sets of tetrahedral angles found for different experiments on the $W_0 = 15.0$ sample in the hexagonal phase. For a tetrahedral arrangement of four cylinders oriented at angles θ_i, the relation $\sum_{i=1}^{4} P_2(\cos(\theta_i)) = 0$ holds, hence (from eq 1) the quadrupolar splittings must sum to zero. Each set of angles shown corresponds to four doublet splittings (with appropriate choice of sign) that sum to zero.

• Cooling from the micellar phase produces a hexagonal phase that is not a random powder. The $W_0 = 23.0$ sample confined in the narrow space between inner and outer glass walls has the appearance of a 2-D powder consistent with cylinder axes being constrained to lie along the glass walls. In the absence of ordering caused by shear, the $W_0 = 15.0$ samples (when cooled through the cubic phase, independent of glass wall separation) give a pseudopowder spectrum indicating a preference for a limited number of domain directions, with the directions changing each time the experiment is repeated.

The first two observations are completely consistent with the picture of the hexagonal phase being composed of cylinders whose axes become oriented in the shear direction. There is a lot of self-consistent evidence supporting this picture.[11,18,23,24]

The structure on cooling from the micellar phase can result from two mechanisms: cylinders preferring an orientation parallel to glass surfaces ($W_0 = 23.0$) and orientation influenced by the intervening cubic phase ($W_0 = 15.0$). Hexagonal-phase pseudopowder spectra have not been observed in the $W_0 = 23.0$ sample, which does not have a higher-temperature cubic phase; this result is consistent with the optical observation of needles in the hexagonal phase formed from a higher-temperature cubic phase.[6]

The splittings observed in the hexagonal phase after passing through the cubic phase report on directions of the cylinders in the cubic phase and are consistent with the hexagonal phase growing from the preferred directions of the cubic phase. The presence of a limited number of doublets in the hexagonal phase indicates that the cubic phase consists of a limited number of crystallites. Rapid shear in the cubic phase does produce somewhat random orientations in the hexagonal phase, but the pattern obtained is not that of a true random powder (Figure 12D).

4.2. Structure of the Lamellar Phase. In the lamellar phase, we notice the following:

• Parallel shear applied to both the $W_0 = 15.0$ and 7.8 samples in the lamellar phase results in well-ordered samples with all domain directors aligned perpendicular to B_0.

• Perpendicular shear produces samples that have a distribution of angles θ with $\theta = 90°$ favored over other angles.

• The doublet splitting in the $W_0 = 15.0$ lamellar phase is roughly equal to the splitting for the same domain orientation in the lower-temperature hexagonal phase. This result is surprising because the reduction in splitting of $P_2(\cos \beta) = -(1/2)$ resulting

from D_2O diffusion around the cylinders of the hexagonal phase does not apply to a lamellar phase that consists of simple planar sheets. With the reasonable assumption that the D_2O order parameter has not changed much from the lower-temperature hexagonal-phase value, the splitting in the lamellar phase is roughly one-half the value one would expect of simple planar sheets. It has been shown that temperature-dependent splittings in a single phase change by $5-20\%$ over a $20°$ interval;[4,29] hence, the almost exact factor of 2 change must arise from a geometric origin.

• It has been suggested[7] that the lamellar phase contains cylindrical defects. This is indeed consistent with the memory effects seen in Figure 10, wherein shear in the lamellar phase produces orientational order in the hexagonal phase. The cylinder direction in the lamellar phase becomes one of the cylinder directions of the cubic phase, and consequently one of the cylinder directions of the hexagonal phase.

• The D_2O splitting becomes smaller with increasing temperature in the $W_0 = 7.8$ sample (Figure 5) and larger in the $W_0 = 15.0$ sample.

The lamellar-phase results summarized above indicate that shear produces oriented domains with directors (layer normals) that are perpendicular to the direction of shear. In the case of parallel shear, this results in layer normals all being perpendicular to B_0. However, the peak splitting is only half that predicted from the lower-temperature hexagonal phase. We first discuss the small peak splittings followed by the spectral patterns observed with perpendicular shear.

4.2.1. Factor of $^1/_2$ Anomaly in Lamellar-Phase Splitting. The small spectral splittings observed in the lamellar phase must be related to deviations from simple planar sheets. Relaxation studies[24] have shown that the lamellar planes have undulations, and diffusion along an undulating surface would reduce the water order parameter. This reduction is unlikely to be sufficient to explain the factor of $^1/_2$.

Imbedded cylinders present a further possibility for splitting reduction. However, the presence of a hexagonal array of imbedded cylinders (as proposed in ref 7) does not in itself lead to a reduced splitting for parallel shear because the surface normals of both the lamellar layers and the cylinder surfaces are then expected to lie perpendicular to B_0 ($\theta = 0°$, $\beta = 90°$ for the cylinders and $\theta = 90°$, $\beta = 0°$ for the lamellar layers). In addition, the maximum splitting for D_2O diffusing around a cylinder is for cylinders aligned parallel to B_0 ($\theta = 0°$) that have their surface planes perpendicular to B_0. The splitting is reduced by $|-(^1/_2)|$ for cylinders with axes perpendicular to B_0 ($\theta = 90°$, eq 3). Hence, the presence of imbedded cylinders, assuming that they are aligned along the shear direction, would be expected on average to reduce the $\theta = 90°$ splitting on going from from parallel ($\theta = 0°$) to perpendicular ($\theta = 90°$) shear. No reduction is observed.

One possibility is that the presence of the cylinders leads to a decrease in the total surface area available to the water. If the presence of the cylinders causes the reduction in D_2O splitting, then the hexagonal packing of the cylinders must be achieved with rather less water than that involved in the normal hexagonal phase or in the packing of the lamellar layers themselves. This explanation would require a factor of roughly 2 decrease in the fraction of surface-associated water, and such a decrease is unlikely.

Defects have often been observed in lamellar phases; structures that have been proposed to explain these defects include bilayers perforated by aqueous pores and bilayers composed of ribbonlike
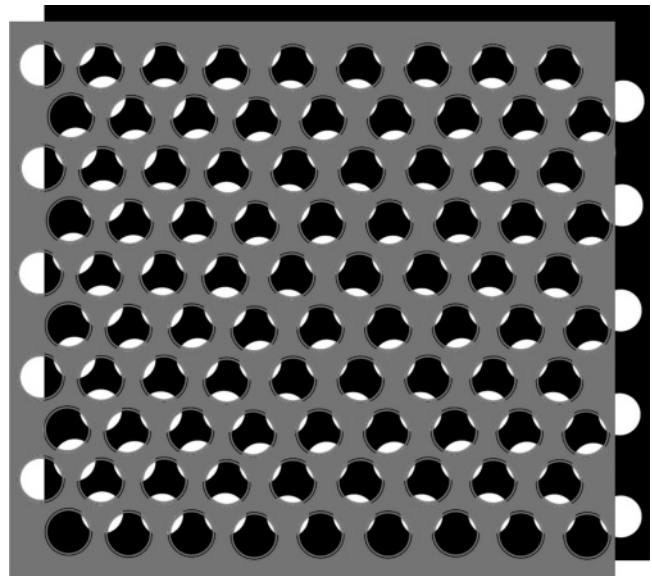

Figure 16. Cartoon of two lamellae in a pore-filled lamellar phase. The hexagonal arrangement of pores is chosen as one that is consistent with X-ray scattering observations of refs 6 and 7. This picture accounts well for observed memory effects. In the presence of shear, one of the three lines of pores could align along the shear direction, preserving the memory of the shear without affecting the lamellar-phase signal but affecting the hexagonal-phase signal in a subsequent quench.

aggregates.[30] An appealing possibility is that the lamellar planes of $C_{12}E_6$ contain cylindrical holes or pores filled with D_2O as shown in a cartoon of two lamellae (colored gray and black) of the proposed structure (Figure 16). Such holes have been suggested for other lyotropic systems[9] and cannot be ruled out for $C_{12}E_6$.[29] Because the surface of the pores has the same effect on the D_2O signal as do the cylinders of the hexagonal phase (reducing the splitting by $|-(^1/_2)|$), the observed signal (with rapid exchange between plane and pore regions) would be an average over the fraction f of D_2O molecules next to the lamellar plane and the fraction $(1 - f)$ of the water next to the pore surfaces

$$\frac{\Delta\nu}{\Delta\nu(\text{lamellar plane})} = \left(f - \frac{1}{2}(1-f)\right) = \frac{3}{2}f - \frac{1}{2} \quad (5)$$

If the fraction of water next to the lamellar plane part is $f = ^2/_3$, then we get the observed splitting reduction (compared to that expected for a simple planar lamellar phase based on the hexagonal-phase value) of $^1/_2$.

One arrangement of pores that is consistent with the scattering experiments[7] is to have them arranged in a hexagonal 2-D array in the lamellar plane (Figure 16). The pores of the adjacent lamellar layer need not register with the first layer; indeed, layers might pack in the aba hexagonal arrangement of cubic close packing (every second layer is in the register). Each layer is 4.8 nm thick.[7] Let us assume that slice 2 has holes that are displaced in the Y direction from slice 1 by (4.8 nm)* $\sqrt{3}$. Slice 3 is similarly displaced with respect to slice 2 and is thus in registry with slice 1. There are now continuous planar strips or regions (in the three directions that are consistent with the hexagonal arrangement of pores, running between the pores) that stack in a hexagonal array and could explain the scattering results. These directions are potentially related to the cylinder directions of the cubic phase, and the pores can be thought of as resulting from the collapse

(29) Sallen, L.; Sotta, P.; Oswald, P. *J. Phys. Chem. B* **1997**, *101*, 4875.

(30) Quist, P.-O.; Halle, B. *Phys. Rev. E* **1993**, *47*, 3374.

of the cubic phase where the interconnected cylinders form layers with holes. Support for this picture comes from diffusion experiments that estimate that the distance between interconnects in the cubic phase is 4.6 nm.[11] This is precisely the lamellar-phase spacing found in the scattering experiments.

Note that the stacking and arrangement of the circles could change under shear without affecting the lamellar-phase splitting. This change could affect the subsequent quench through the cubic into the hexagonal phase.

The picture that emerges is that the D_2O is sampling both planar and pore regions leading to a reduced spectral splitting compared to that expected from the lower-temperature hexagonal-phase splitting. Rançon and Charvolin[7] suggested that the increased splitting with increasing temperature in the lamellar phase is associated with a reduction in the number of imbedded cylinders as one approaches the micellar phase. A decrease with increasing temperature in the number and/or size of pores would have the same effect.

4.2.2. Powder Patterns Resulting from Perpendicular Shear in the Lamellar Phase of the $W_0 = 15.0$ (Four-Phase) Sample. Whereas parallel shear produces a distinct doublet indicating that all domains are perpendicular to B_0, perpendicular shear produces a distorted powder with preference for domains oriented perpendicular to B_0 but with a substantial portion of the signal coming from domains oriented in other directions, including parallel to B_0. In some cases (not shown), there is a rather large parallel component. This is especially true for the $W_0 = 15.0$ sample for which rapid shear near the lamellar/micellar transition temperature leads to both perpendicular and parallel peaks whereas slow shear gives perpendicular peaks only.

Our results are consistent with the observations of Lukaschek et al.,[15] who applied shear to the lamellar phase of $C_{12}E_6/D_2O$ in a plane perpendicular to B_0. They find that slow shear orients much of the sample with normals parallel to B_0 (equivalent to the perpendicular signal in our experiments) whereas faster shear increases the fraction of sample with directors perpendicular to B_0 (equivalent to the parallel signal in our perpendicular-shear experiments and to the parallal hexagonal-phase signal in Figure 10F that results when cooling a sample that was subjected to perpendicular shear in the lamellar phase).

We emphasize that the $\theta = 0°$ signal must arise from planes that have their normals parallel to B_0 while at the same time all normals are perpendicular to the shear direction (as required by the parallel shear result). Hence the lamellar phase involves regions (crystallites) that align with normals perpendicular to the shear direction. Slow perpendicular shear might align most of the crystallites with plane normals perpendicular to B_0 (parallel to the shear gradient direction), and rapid shear might result in a more-or-less 2-D powder where $\theta = 90°$ (normals parallel to the shear gradient direction) and $\theta = 0°$ (normals perpendicular to both the shear gradient and shear directions, i.e., parallel to the vortex direction) are both found for layer normals. Such a model would explain the growth of the parallel component observed with rapid shear near the lamellar/micellar phase transition and is consistent with earlier results on the $C_{12}E_6/D_2O$ system.[15] It would also explain the presence of both parallel and perpendicular peaks in the hexagonal phase (Figure 10) after cooling following parallel (E) or perpendicular (F) shear in the lamellar phase.

One possible model to explain the distorted powder signal resulting from perpendicular shear in the lamellar phase is the onionskin structure found for the lamellar phase of phospholipids. If the cylinders should consist of sheets wrapped around to form concentric cylinders of radii large enough to avoid motional

narrowing by D_2O diffusion between areas of differing θ, then a powder signal including intensity at $\theta = 0°$ would result if such concentric cylindrical structures were oriented by perpendicular shear. In the case of $C_{12}E_4/D_2O$, onionskin structures are claimed to explain the isotropic NMR peak found for high shear rates.[15,16] The isotropic peak indicates that these structures are roughly spherical and thus would be unable to explain our observations.

Another model that is consistent with the observations is a lamellar phase composed of ribbons[30] (containing pores) that are flat for a sufficient length that the D_2O doublet is not motionally narrowed by diffusion among regions with different layer orientations. The ribbons would have their long axes oriented by shear with a distribution of normal directions distributed about the shear direction. Hence perpendicular shear would produce some ribbons with layer normals parallel to B_0 giving the $\theta = 0°$ signal.

The lamellar planes (of ribbons or crystallites) could change orientation over long length scales and could have continuous planar directions between pores that would likely be aligned by shear. This alignment would explain the result that parallel orientation from shear in the lamellar phase gives a parallel-oriented hexagonal-phase signal upon cooling to the hexagonal phase through the cubic phase (Figure 10E). However, without shear in the lamellar phase a pseudopowder pattern of multiple peaks is obtained. This picture is consistent with the continuous directions in the lamellar phase and the cylinders in the hexagonal-phase structures being related to one of the cylinder directions of the cubic-phase structure depicted in Figure 9. In this picture, the significant intensity between the 90° hexagonal-phase peaks in Figure 10E results from other directions involved in the cubic structure.

It is clear that any model must involve layer normals aligning perpendicular to the shear direction, with a distribution of normals about the shear direction. The proposed pore model is akin (at least locally) to the onionskin, ribbon, and crystallite models except that the addition of holes (consistent with diffusion experiments with tracer molecules[9]) allows us to rationalize the value of the lamellar-phase splitting. The patterning of holes in the structure might also explain the shear memory upon subsequent quenching into the hexagonal phase.

4.3. Structure of the Cubic Phase and Memory across Phase Transitions. Deuteron NMR does not give any direct information about the cubic phase, except that it is NMR-isotropic. However, recent diffusion measurements[11] agree with ref 7 and suggest strongly that the cubic phase is composed of interconnecting rods arranged in an *Ia3d* structure (Figure 9).

An interesting feature of the cubic phase is that the orientations of oriented hexagonal- and lamellar-phase samples are maintained when passing through (by changing temperature) the NMR-isotropic cubic phase. As the cubic phase grows from the hexagonal or the lamellar phase, one of the cylinder directions of the cubic phase grows from the cylinder or planar strip direction of the other phase; and as the hexagonal or lamellar phase grows from the cubic phase, the cylinders or planar strips align along one of the directions of the cubic cylinders. Hence, the cylinder orientations dictate the direction of growth of the new phase, leading to memory across phase boundaries. As proposed by Rançon and Charvolin,[6,7] heating an oriented hexagonal phase into the cubic phase preserves the orientation direction as *one* of the directions of rod orientation on the *Ia3d* lattice. The same idea applies to the lamellar phase, which is known to contain cylinders (or planar strips) imbedded in the lamellar layers.

5. Conclusions

We have presented results of NMR experiments on D_2O in $C_{12}E_6/D_2O$ lyotropic mesophases. In all cases, shear orients the hexagonal phase with the cylinder axes along the shear direction. In samples that do not have intermediate cubic and lamellar phases, cooling a thin hexagonal-phase sample yields a 2-D powder with cylinder axes aligned along the glass surfaces. Samples with intermediate cubic and lamellar phases often give rise to a limited number of crystallites in the hexagonal phase; the splittings are explained by tetrahedral arrangements of hexagonal directors indicating that the hexagonal crystallites grow from the tetrahedral directions of the cubic phase.

Parallel shear orients lamellar-phase plane normals perpendicular to B_0, and perpendicular shear shows that there is a distribution of these layer normals perpendicular to the shear direction. With low shear rates, the preference is for the planes to have their normals lying in the shear gradient direction. These results are consistent with the lamellar phase being composed of ribbons or with lamellar regions where the director takes more or less random directions that are perpendicular to the shear direction. The continuous planar regions (between pores) of the lamellar phase lie along the shear direction and thus along the ribbon axis (if ribbons exist). These regions grow from the tetrahedral directions of the cubic phase. A picture that is consistent with the results is that the cubic-to-lamellar phase transition involves the interconnected tetrahedral cylinders of the cubic phase collapsing to form layers with holes (pores), the cubic cylinder directions becoming the continuous planar (between holes) regions of the lamellar phase.

The lamellar-phase splittings are half that expected on the basis of the splittings observed in the lower-temperature hexagonal phase and increase with temperature. This decreased splitting results from pores that span the lamellar layers. The increase in splitting with increasing temperature results from the decrease in the number and/or size of the pores at higher temperature.

There is orientational memory across phase boundaries (from lamellar to hexagonal phase and vice versa); the additional orientations that always accompany such phase transitions are consistent with the four tetrahedral orientations of the cubic phase from which the lamellar or hexagonal phase grows. As argued from X-ray and neutron-scattering experiments,[7] these results show that the lamellar- and hexagonal-phase structures are related to the cubic-phase structure from which they grow.